ISBN: 978-3-95450-247-9 ISSN: 2673-5490 doi: 10.18429/JACoW-IPAC2024-WEPC79

THE DESIGN OF A 2.3-CELL X-BAND PHOTOCATHODE RF ELECTRON GUN

Zixin Guo, Haoran Zhang, Biaobin Li, Xiazhen Xu, Jingya Li, Zhigang He*,
Shancai Zhang, Lin Wang, National Synchrotron Radiation Laboratory,
University of Science and Technology of China, Hefei, Anhui, 230029, China

Abstract

Recent advancements in electron beam compression methods have enabled the production of ultrashort electron beams at the sub-femtosecond scale, significantly expanding their applications. However, the temporal resolution of these beams is primarily limited by the flight time jitter, especially during their generation in photocathode RF electron guns. In this paper, to mitigate the impact of microwave phase jitter on the flight time jitter inside the electron gun, we designed a 2.3-cell X-band electron gun, which enables the electron beams to acquire maximum output energy and minimum in-gun flight time at the same injection phase. Moreover, the tolerance of the cavity's machining errors is assessed and the RF input coupler of this cavity has been designed. Our simulation results indicate that this design provides a solid foundation for further improving the temporal resolution of the electron beam.

INTRODUCTION

Ultrashort electron beams are essential for probing the ultrafast dynamics of matter and are fundamental to ultrafast electron microscopy techniques. Although significant advancements in bunch compression technology have enabled the production of electron beam with sub-femtosecond time scales, its temporal resolution remains constrained by the flight time jitter. To suppress the flight time jitter, both the double-bend achromatic (DBA) method in magnetic bunch compression schemes [1, 2] and the bunch energy chirp control method [3] in optical bunch compression schemes have been proposed as solutions to mitigate the flight time jitter caused by the differences in the average energy of electron beams.

However, these methods for mitigating time jitter are based on the dynamics of relativistic electron beams, not considering the complex dynamics during the acceleration of electron beams to relativistic energies within the electron gun. In particular, the microwave phase jitter within the Rf cavity can greatly affect the electron beam's output energy and the in-gun flight time. To solve this problem, a 2.3-cell photocathode electron gun with a structure of 0.4:0.9:1 has been proposed and validated in the S-band [1]. This cavity can simultaneously allow the electron beam to gain the maximum output energy and the minimum in-gun flight time at the same injection phase.

To adapt this 2.3-cell structure for the method that control the energy chirp of electron beams to mitigate flight time jitter, it is essential for the energy chirp to range from 100 to 200 MeV/m, a requirement that exceeds the capabilities of S-band electron guns. Therefore, in order to achieve the necessary energy chirp, this cavity must be specifically engineered for operation in the X-band [3]. In this paper, we first designed the structure of this cavity, which operates at 11.424 GHz. Subsequently, we explored the dynamics of electron beams across different injection phases and assessed the potential effects of machining errors on the RF parameters and beam dynamics. Finally, we also designed a dual-feed coupling slot for this cavity to enhance RF power input efficiency.

DESIGN OF THE RF CAVITY

As shown in Fig. 1(a), the 2.3-cell photocathode RF electron gun consists of three cells, with a structure of 0.4:0.9:1. Unlike traditional BNL-type cavities, the profile of this RF cavity uses a combination of circular and elliptical shapes instead of the rectangular pillbox design. This design effectively enhances the volume-to-surface-area ratio of the cavity, thereby increasing its quality factor Q_0, and ensures more uniform microwave heating, which is advantageous for the development of subsequent cooling systems.

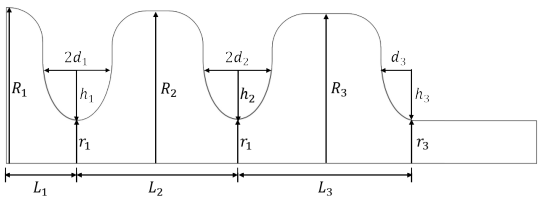

Figure 1: Schematic diagram of the 2.3-cell photocathode RF electron gun.

In the design, the initial step is to determine the lengths of the three cells (L_1, L_2, L_3), which can be calculated by multiplying their structural ratios by $L_{Fullcell} = 0.5 \times c/f = 13.12\ mm$,with c representing the speed of light and f representing the operating frequency. Subsequent steps mainly focus on determining the radius of each cell (R_1, R_2, R_3), which may influence the RF cavity's operating frequency and field flat ratio. Finally, the radius (r_1, r_2, r_3), widths ($2d_1$, $2d_2$, d_3) and curvatures (h_1, h_2, h_3) of the coupling holes between each cell should be optimized, based on the factors such as the quality factor Q_0, mode separation Δf. We have simulated this cavity in POISSON SUPERFISH and list its main parameters Table 1. The

* hezhg@ustc.edu.cn

ISBN: 978-3-95450-247-9 ISSN: 2673-5490 doi: 10.18429/JACoW-IPAC2024-WEPC79

normalized longitudinal electric field E_z along the axis of this electron gun can also be obtained, as illustrated in Fig. 2.

Table 1: RF Gun Parameters

Parameter	Value
Cells	2.3
$f_{\pi-mode}$	11.4241 GHz
f_{0-mode}	11.3667 GHz
Mode Separation Δf	57.3 MHz
Quality Factor Q_0	7880
Field Flat Ratio	1.02

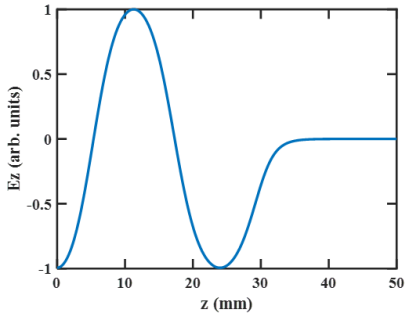

Figure 2: The normalized longitudinal electric field E_z along the axis of this electron gun.

ANALYSIS OF BEAM DYNAMICS

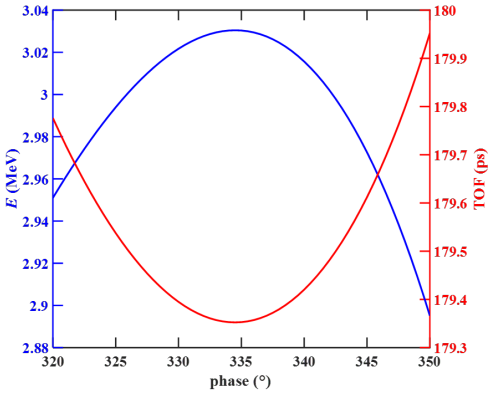

Figure 3: Beam dynamics under different injection phase.

To assess the dynamics of the electron beam inside this electron gun, we conduct simulation study using the particle simulation software General Particle Tracer [4]. In the simulation, the electron beam has a charge of 10 fC, with the driving laser of 50 fs pulse width (uniform) and 50 µm radius (uniform). When the amplitude of the longitudinal electric field is set to 190 MV/m, the beam dynamics under different injection phases are displayed in Fig. 3. Notably, at an injection phase of 334.5°, the electron beam achieves the maximum output energy (E) and the minimum in-gun flight time (TOF). Moreover, maintaining the phase jitter within ±0.5° ensures that the beam dynamics remain stable, thus significantly reducing the effects of phase jitter.

TOLERANCE ANALYSIS OF THE CAVITY

During the manufacturing process of this cavity, machining errors are inevitable, resulting in differences between the actual RF performance and the designed value. Therefore, it is necessary to analyze its machining errors and establish reasonable tolerance limits. Moreover, the machining errors can be classified into dimensional errors and shape errors.

To assess the impact of dimensional errors, we assume a variation of 1 µm in each dimensional parameter of this cavity. Simulation results indicate that dimensional errors primarily affect the operating frequency of the cavity, leading to a frequency shift f_{shift}, as shown in Table 2. It is evident that the most frequency-sensitive parameters are the radius of each cell (R_1, R_2, R_3), followed by the widths of the coupling holes between the cells (d_1 and d_2). Therefore, the tolerance requirements for these parameters must be the strictest in subsequent manufacturing processes, while less sensitive parameters may have more relaxed tolerance standards.

Table 2: Frequency Shift caused by 1 µm Dimensional Error

Parameter	Frequency shift f_{shift} (MHz)
R_1	0.29
R_2	0.38
R_3	0.34
r_1	0.03
r_2	0.06
r_3	0.05
d_1	0.22
d_2	0.17
d_3	0.10
h_1	0.05
h_2	0.06
h_3	0.01

Shape errors primarily relate to deviations that disrupt the cylindrical symmetry of the cavity. These errors include non-uniform roundness of each cell, misalignments in coaxial alignment between cells, and variations in the tilt angle of the whole cavity during machining and assembling processes. Once the cylindrical symmetry is disrupted, harmful higher-order modes such as dipole and quadrupole fields will emerge, affecting the dynamics of the electron beam. To evaluate the impact of these shape errors, we considered coaxial misalignments between cells of 1 µm, 5 µm, and 10 µm, and tilt angles of 1 mrad, 5 mrad, and 10 mrad, respectively. Simulation results indicate that coaxial misalignments between cells have a minimal impact on the dynamics of the electron beam. However, the tilt angles of the whole cav-

ISBN: 978-3-95450-247-9 ISSN: 2673-5490 doi: 10.18429/JACoW-IPAC2024-WEPC79

ity significantly affect the in-gun flight time of the electron beam, as shown in Fig. 4. This figure illustrates that as the tilt angle increases, the time it takes for the electron beam to pass through the cavity increases, and the maximum output energy decreases. This is mainly because that the tilt angle introduces dipole fields, which gradually cause the electron beam to deviate from the center axis where the acceleration gradient is greatest. As a result, the beam with lower energy must traverse a longer path to reach the exit of the electron gun, which can also be evidenced by the offset of beam's transverse center at the gun exit. When the tilt angle is 1 mrad (equivalent to a height difference of 50 µm between the longitudinal beginning and end of the electron gun), the optimal injection phase remains at 334.5°. At a tilt angle of 5 mrad, the optimal injection phase should be adjusted to 333.5°. However, when the tilt angle reaches 10 mrad, the phase for maximum energy injection is 332.5° and the phase for the shortest flight time is 333.5°, a discrepancy that no longer meets the initial design requirements. Additionally, as the tilt angle increases, the energy chirp of the electron beam will decrease to some extent.

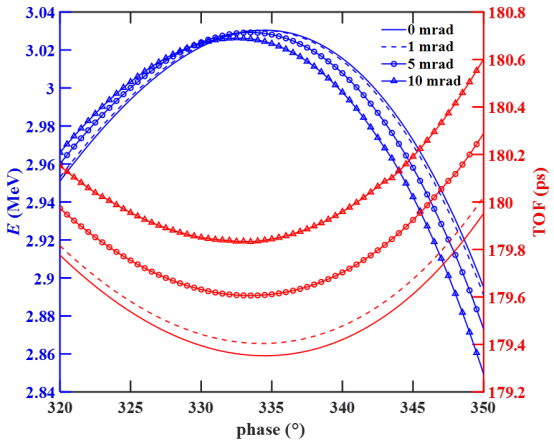

Figure 4: Beam dynamics under different tilt angles of the whole cavity.

DESIGN OF THE POWER INPUT COUPLER

Coupling RF power into the cavity efficiently is essential in the design of photocathode RF electron guns. In our design, we utilized the widely used slot coupling method for the coupling system. Additionally, to minimize the disruption of cavity symmetry caused by the coupling slot, we adopted a dual-feed power input scheme. The schematic of this input coupler is depicted in Fig. 5. The Two coupling slots are positioned at the top and bottom of the third cell, with their lengths, widths, and heights specified as l_c, w_c, h_c respectively. These slots are connected to the standard waveguide WR75 to facilitate the feeding of X-band RF power. By adjusting the dimensional parameters of the slots, it is possible to achieve impedance matching between the coupling slots and the cavity, thus enabling low-reflection RF energy input. The S_{11} parameters of the input coupler is demonstrated in Fig. 6, displaying a reflection factor of -34 dB at 11.424 GHz.

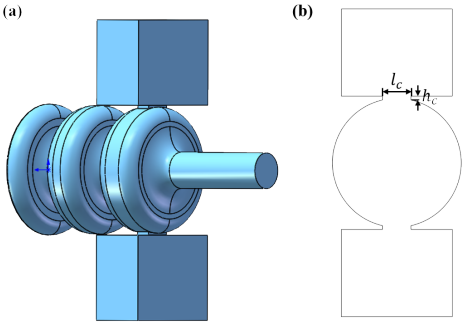

Figure 5: Schematic of the input coupler: (a) shows the 3D view and (b) displays the 2D cross-section view.

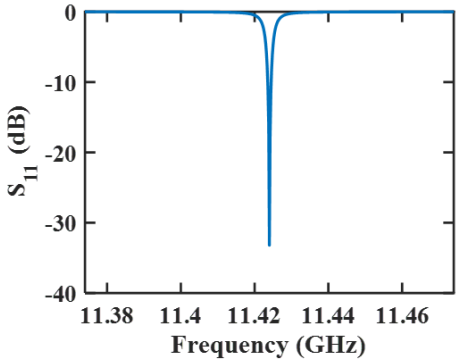

Figure 6: S_{11} parameters of the input coupler.

Additionally, it is important to note that the introduction of coupling slots may cause a shift in the operating frequency of the cavity and change the field flat ratio to some extent. Therefore, after the initial design of the coupling slots, further optimization of the cavity's structural parameters is required. Through the iterative design of the cavity and coupler, the specific dimensions of the coupling slots can be finally determined.

CONCLUSION

For the 2.3-cell photocathode RF electron gun operating in the X-band (11.424 GHz), we have completed the preliminary design and determined its structure parameters. Through the analysis of beam dynamics, we have assessed its tolerance of manufacturing errors. Additionally, we designed a dual-feed coupler to achieve low-reflection RF power input. Our future work will incorporate thermal analysis to further refine and optimize the design of the electron gun.

ACKNOWLEDGEMENTS

This work is supported by the Youth Innovation Promotion Association (CAS).

ISBN: 978-3-95450-247-9 ISSN: 2673-5490 doi: 10.18429/JACoW-IPAC2024-WEPC79

REFERENCES

[1] F. Qi *et al.*, "Breaking 50 femtosecond resolution barrier in MeV ultrafast electron diffraction with a double bend achromat compressor", *Phys. Rev. Lett.*, vol. 124, no. 13, p. 134803, 2020. doi:10.1103/PhysRevLett.124.134803

[2] H. W. Kim *et al.*, "Towards jitter-free ultrafast electron diffraction technology", *Nat. Photonics*, vol. 14, no. 4, pp. 245-249. doi:10.1038/s41566-019-0566-4

[3] Z. Guo *et al.*, "Ultrashort electron bunches with subfemtosecond jitter from an *X*-band photocathode rf gun", *Phys. Rev. Accel. Beams*, vol. 26, p. 123401, 2023. doi:10.1103/PhysRevAccelBeams.26.123401

[4] M. J. de Loos and S. B. van der Geer, "General Particle Tracer: A New 3D Code for Accelerator and Beamline Design", in *Proc. EPAC'96*, Sitges, Spain, Jun. 1996, paper THP001G, pp. 1241–1243.